Growth and Characterization of Ternary and Quaternary Wide Gap II-VI Quantum Wells and Nanostructures

H. Sitter

Institute for Semiconductor and Solid State Physics, Johannes Kepler Universität Linz,

Altenbergerstr. 69, A-4040 Linz, Austria

E-mail: Helmut.Sitter@jk..uni-linz.ac.at

The wide gap II-VI compound semiconductors are well known as promising materials for optoelectronic devices in the blue green spectral range. In this paper we review the activities in this field at the Johannes Kepler University in Linz. We will report on the growth of ternary and quaternary II-VI compounds by Molecular Beam Epitaxy and Atomic Layer Epitaxy to obtain quantum wells and light emitting diodes. The second way to obtain quantum confinement effects is to fabricate nanostructures by reactive ion etching, which was realized in a plate reactor. The in situ characterization during growth was performed by reflection high energy diffraction and Auger electron spectroscopy. The ex situ characterization of the layers as well of the etched structures was done by high resolution x-ray diffraction, photoluminescence and electroluminescence.

1. Introduction

The binary and ternary II-VI compound semiconductors are applicable to the production of blue light emitting diodes, which are based on lattice matched multilayer structures [1-3].

An optimized layer structure can only be designed if the band offsets between the different materials are well known. Therefore we investigated carefully the band offset transition of the ZnMgSe-ZnTe system [4]. Based on that knowledge ZnCdSe/ZnMgSe quantum wells could be fabricated with well defined optical properties [5]. For the growth of light emitting diodes also the n- and p-type doping problem had to be solved, which was achieved by a nitrogen DC-plasma source together with a superlattice structure [6]. To fulfill the optical and electrical confinement conditions quaternary ZnMgSeTe layers were used to obtain light emitting diodes in the blue spectral range[7,8].

Using a CH_4/H_2 reactive ion etching (RIE) technique the grown quantum wells could be further reduced in there dimensionality[9]. But in contrast to the expectations a red shift in the photoluminescence spectrum was observed, which can be explained by strain relaxation overwhelming the effect of confinement. The influence of strain on the layer structures was investigated intensively by high resolution x-ray diffraction (HRX) [10].

All effects described above are very sensitive to the composition of the active layers and surfaces involved. Therefore we emphasized the control of the surface composition by quantitative Auger electron spectroscopy (AES) during the growth as well as after any chemical treatment as for example by RIE [11,12].

2. Experimental

The epitaxial growth of ternary and quaternary II-VI compound layers on GaAs substrates was performed in a vertical molecular beam epitaxy (MBE) chamber [13]. The growth chamber is equipped with Cd, Zn, Mg, and Te effusion cells and with a Se-cracker cell. For doping the layers during growth a $ZnCl_2$ source for n-type and a nitrogen DC plasma source for p-type are also installed in the growth chamber. The vertical arrangement of the growth chamber in combination with a special design of shutter allowed to grow the layers either in the MBE mode or in the atomic layer epitaxy mode [13].

In situ control of the two dimensional growth process was performed by reflection high energy electron diffraction (RHEED) and laser interferometry. An analysis chamber is connected with the growth chamber by an ultra high vacuum transfer system. That makes it possible to transfer the samples from the MBE chamber to the scanning Auger spectrometer for surface analysis.

The preparation of the quantum wires and quantum dots was done in a plate reactor for RIE in a CH_4/H_2 gas mixture.

The ex situ characterization was made by photoluminescence (PL), electroluminescence (EL) and HRXD. The electrical properties were investigated by Hall effect measurements.

3. Results

3.1 Quantum well and multilayer structures

3.1.1 ZnMgSe - ZnTe system

To tailor devices, information on the band alignment of the alloy in relation to other compounds is needed. Sofar no experimental data were available for ZnMgTe. Chadi [14] has predicted a lowering of the valence band by some tenth

of an eV. To cheque this prediction, we have grown a series of multi quantum wells of $Zn_{1-x}Mg_xSe/ZnTe$ by MBE (see Fig. 1a) and investigated the optical properties by PL.

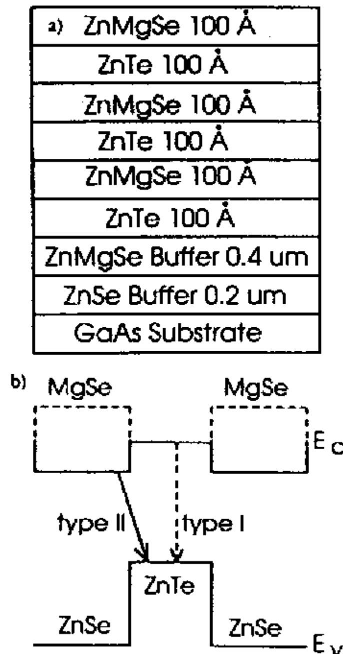

Fig.1. (a) Scheme of the layer structure of the multi-quantum -well samples. (b) Expected band alignment of ZnTe-ZnSe (solid) and ZnTe - MgSe (dashed), showing a transition from a type II (solid arrow) to a type I lineup (dashed arrow).

The idea behind this structure is demonstrated in Fig. 1b. The band alignment for ZnSe/ZnTe is type II, where the optical transition occurs from the conduction band of ZnSe to the valence band of ZnTe. According to the " common anion rule" [15] one would only expect a shift in the conduction band with the addition of Mg. The transition energy must then increase as a function of Mg composition. At higher Mg concentration, the ZnMgSe conduction band will be probably higher than that of ZnTe, and the band alignment will change from Type II to type I. Comparing the increase of the luminescence energy with the increase in bandgap energy of the ZnMgSe alloy one can determine how this energy is distributed between the conduction band and the valence band.

Fig. 2a shows the peak energy of the near band edge emission of $Zn_{1-x}Mg_xSe$ samples plotted as a function of Mg content. The line is a linear fit to the data and gives a bandgap variation of 7.87 meV per percent Mg content in the compound. The energy gap values for ZnSe (2.77 eV) and MgSe (3.55 eV) extrapolated from the fit are smaller than the literature data, 2.82 eV and 3.6 eV respectively. A difference of 10 to 30 meV can by explained by the exciton binding energy for this compound.

The PL data for the multilayer quantum well samples are shown in Fig. 2b, where we plotted the peak energy of the PL spectra versus the Mg content in the $Zn_{1-x}Mg_xSe$ layers. When the Mg content is zero, we get a peak energy of 1.9eV. It corresponds to the type II transition from the conduction band to the ZnTe valence band, considering a valence band offset of 880meV between the ZnTe and ZnSe. As the Mg concentration increases, the PL peak energy shifts to higher values, until about 2.39eV, which corresponds to the gap energy of ZnTe. For x larger than 0.6, the energy of the P peak remains constant. The solid line is a fit to the data. The energy dependence with increasing Mg content is the same as for the $Zn_{1-x}Mg_xSe$ layers, indicating that the addition of Mg shifts only the conduction band upwards. Therefore the $Zn_{1-x}Mg_xSe$ system really obeys the common anion rule, in contrast to the prediction of Chadi . For a Mg concentration of about 6%, the $Zn_{1-x}Mg_xSe$ conduction band reaches the conduction band minimum of ZnTe and there is a transition from a type II to a type I alignment.

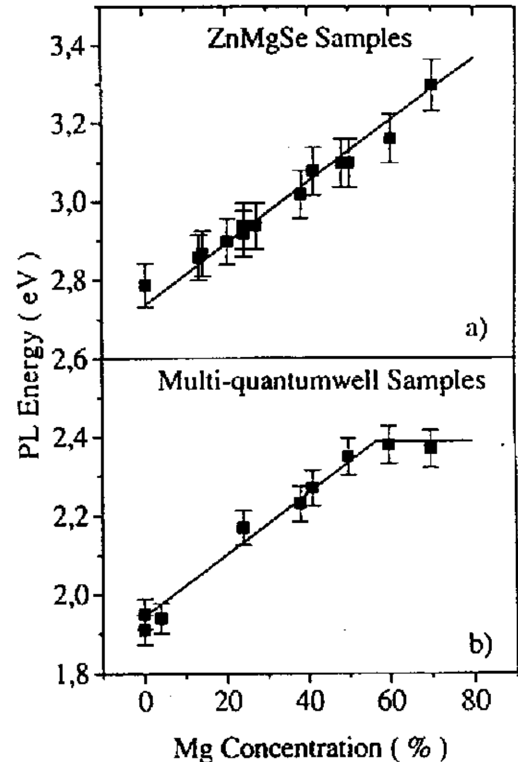

Fig.2. (a) Energy of the near band edge PL data for the ZnMgSe samples as a function of the Mg concentration. (b) PL peak energy for the ZnMgSe/ZnTe multi-quantum-well structures as a function of the Mg content in the well layers.

3.1.2 ZnCdSe - ZnMgSe system

For the optimization of optoelectronic devices, the strain state of the active layer is a very important parameter to be considered, since it influences the band offset and therefore the quantum confinement. ZnCdSe quantum wells are always under compressive strain in ZnSe, however, if such quantum wells are embedded in ZnMgSe the strain can be controlled from compressive to tensile depending on the Cd content in the well.

One advantage of using ZnMgSe instead of ZnSe, is that its band gap energy is 3.05eV for 35% Mg in comparison to 2.82eV for ZnSe. The larger energy leads to a higher confinement and, most important, permits also the use of materials with larger band gap as quantum well in a diode structure. This opens the possibility of making devices emitting in a shorter wavelength. The disadvantage of the corresponding bigger lattice constant can be overcome by

growing a thick buffer layer on GaAs of about 2,5 μm. In addition, the possibility to use unstrained, lattice matched quantum wells, implies that there is no limit in the thickness, and that the device can be freely optimized.

We have grown three series of single quantum well (SQW) samples with a Cd content of 0, 16 and 26%. For each Cd concentration the SQW thickness was 50,75 and 100 Å. Multi-quantumwell (MQW) samples having four quantum wells with different Cd content and thickness of 50 and 100 Å were also grown by MBE.

The Mg content of the barriers was between 35 and 37% as measured by HRXD. The Cd content in the SQW and MQW structures was also determined by HRXD. The PL measurements were performed at 4.2K using an argon laser line at 363.8nm and a power of 50mW.

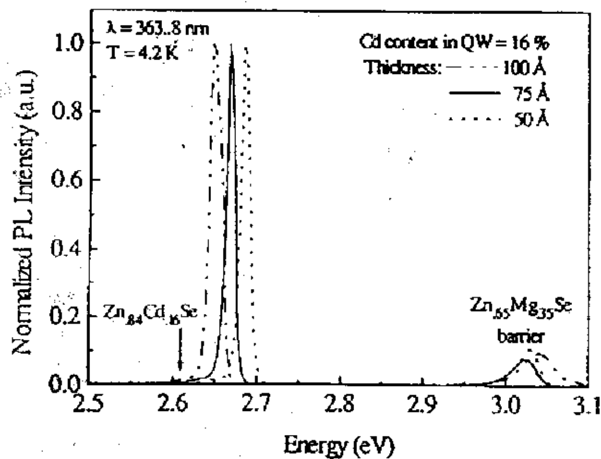

Fig.3. PL spectrum of three SQW samples with 16% Cd and a thickness of 50, 75 and 100 Å.

The normalized PL spectra of the SQW, where the Cd content was 16% are shown in Fig. 3. The thicknesses are indicated in the figure. The small peak around 3.04 eV originates from the ZnMgSe barrier layers. The SQW emissions have a full width at half maximum (FWHM) between 12 and 16 meV and comparable intensity.

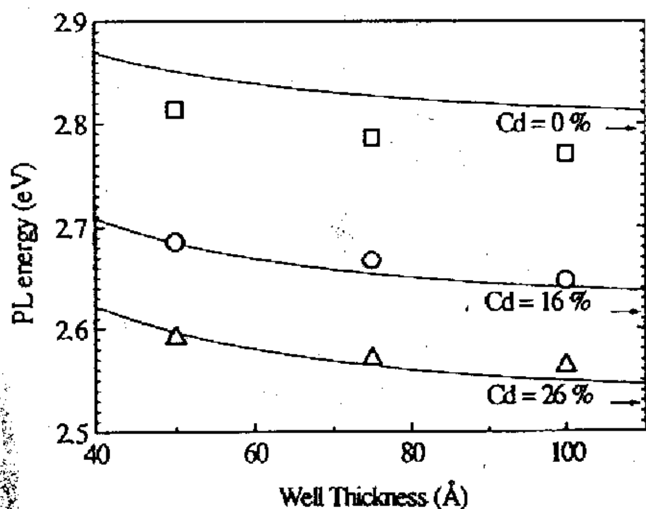

Fig.4. PL peak energy as a function of the thickness for three SQW series. The solid curves are the theoretical calculations and the arrows indicate the measured gap energy for each well material.

The same measurements were done for the SQW's with 0 and 26% Cd. Fig. 4 shows the PL emission energy for the three series of samples as a function of the well thickness, together with a theoretical curve for each case, which was calculated using a simple Kronig-Penny model. Assuming the same excitonic binding energy for all layers, the agreement between data and theory is very good for the SQW with 16 and 26% Cd. The strains are -0.244% (tensile) and 0.383 (compressive), respectively. For the ZnSe SQW, where the strain is much larger, namely 1.351%, the measured energies are 35 to 45 meV smaller than calculated and for two samples even smaller than the ZnSe film PL energy. The discrepancy between experiment and theory is caused by the reduction of the well energy gap due to strain [16].

In order to compare the PL intensities we used the MQW samples, since in that way small differences in the sample quality can be avoided. Fig. 5 shows the PL spectra of the 2 MQW samples. The lower scale gives the energy of the QW emission and the upper axis the strain relative to the barriers. The Cd content is indicated near the corresponding peak. The main point to note in this figure is the small intensity of the ZnSe QW's as compared to ZnCdSe. This behavior can be understood, if we remember that there is no valencband offset between ZnSe and ZnMgSe, as described above. This means, that the valencband confinement for these samples is due only to the increase in the light hole band energy caused by strain. The addition of only 9.5% Cd in the QW produces an increase of 50% in the PL intensity. For the QW with 17% Cd the intensity is 10 times higher. For higher Cd content one would expect an increase in the intensity, since the quantum confinement is larger. This is not the case and there is in fact the tendency to lower intensities. A possible explanation could be an effect of the larger compressive strain, that moves up the conduction band and consequently reduces the confinement.

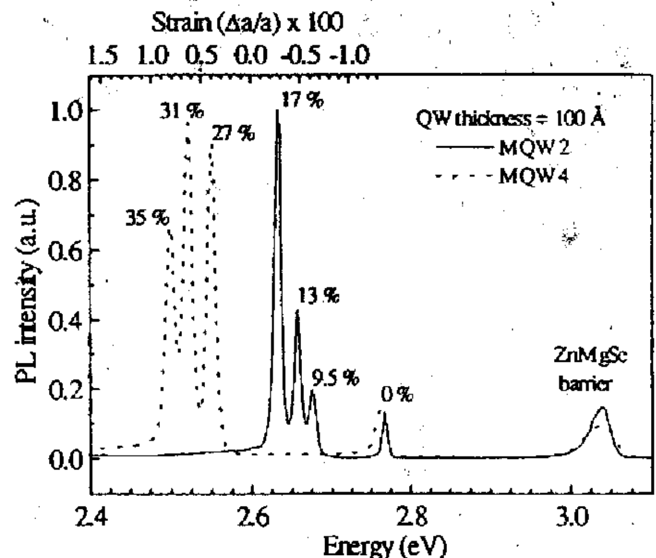

Fig.5. PL spectrum of the MQW samples. The lower axis shows the emission energy and the upper axis the strain of each QW in relation to the barrier. The Cd content for each QW is indicated near the corresponding peak.

3.2 Light emitting diodes

It has been demonstrated that the ZnMgSe ternary compound is a good candidate as an alternative base material for blue laser diodes due to its energy gap and the ability to be doped n-type up to 10^{18} cm^{-3}. [17,18] As described above, ZnCdSe quantum wells (QW), with Cd concentration between 15 and 30 %, embedded in $Zn_{0.65}Mg_{0.35}Se$ barriers exhibit very sharp and intense photoluminescence emissions. At 4.2 K, the PL emission corresponds to energies up to 2.7 eV, for the QWs with 15 % Cd content, but at room temperature the PL peak shifts to lower energies and real blue emission is not possible. The reduction of the Cd content in the QW increases the emission energy, but reduces, at the same time, its intensity, due to the reduction of the valence band confinement. [5]

In the case of ZnSe, it has been shown that the addition of Mg shifts only the conduction band of the ternary compound to higher energies, leaving the position of the valence band unchanged [4]. If the effect is the same for the quaternary ZnMgCdSe, the addition of Mg to the ZnCdSe QW could open the possibility to increase the emission energy without reducing the valence band confinement and, therefore, maintaining the high intensities obtained with the ZnCdSe QWs.

The samples were grown by MBE on (001) GaAs epiready substrates. The growth temperature was 300 °C and the growth rate between 2.0 and 2.5 Å/s. The Zn, Mg, Cd and Se fluxes were adjusted to have a slightly Se stabilized (2x1) surface reconstruction during the growth process, as observed by RHEED.

After calibrating the cell temperature necessary to obtain a planned Cd concentration, a series of samples containing quaternary QWs have been grown. The sample structure consists of a 0.1µm thick ZnSe buffer, a 0.5µm thick $Zn_{0.65}Mg_{0.35}Se$ barrier, a 60Å ZnMgCdSe QW and a 0.1µm thick $Zn_{0.65}Mg_{0.35}Se$ cap layer. The Cd content of the QW was increased from 10 to 37 %. Fig. 6 shows the PL spectra at 77 K of three ZnMgCdSe QW samples. The intensity of the PL signal increases at the same time that the peak energy shifts to lower values when the Cd concentration increases. This is due to the larger confinement in the QW when the energy gap of the quaternary alloy decreases. Comparing with the ZnCdSe QWs with identical structure reported in chapter 3.1.2, the emission energies are much higher for the ZnMgCdSe QWs, due to the larger band gap caused by the addition of Mg. The emission of the QW with 37 % Cd is about 2.6 eV, instead of less than 2.5 eV for the ZnCdSe QW with the same Cd content.

The intensity of the PL emission of the quaternary QWs is comparable with the intensity of the ZnCdSe QWs with the same Cd content, although the total confinement is smaller. This indicates that, as expected, the effect of Mg addition is mainly in the conduction band and the hole confinement produced by the addition of Cd is the main factor controlling the emission intensity. The FWHM of the PL peaks is about 30 meV as indicated in the Fig. 6. It is important to note that these measurements were made at 77.5 K. At 4.2 K, these samples show a peak width of between 11 and 16 meV, which is approximately 2 times larger than that obtained for our best ternary ZnCdSe QWs.

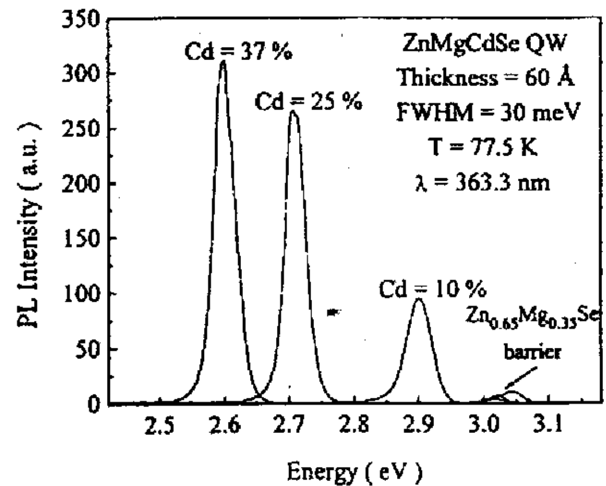

Fig.6. PL spectrum of three ZnMgCdSe QW samples with 10, 25 and 37% Cd. The Zn to Mg ratio is 65 to 35 and the QW thickness is 60 Å for each sample.

Finally, light emitting diodes containing these quaternary QWs were fabricated. The structure of the diodes is shown in the Fig. 7, together with a band diagram under flat band conditions. The n-type side of the diode is formed by a graded ZnMgSe buffer layer, where the Mg concentration increases linearly from 0 to 35 %. The total thickness of this layer is about 0.5 µm and it is followed by a 1.5µm thick $Zn_{0.65}Mg_{0.35}Se$ layer. These two layers were doped n-type to about 10^{18} cm^{-3} using $ZnCl_2$, as described in the ref. 18.

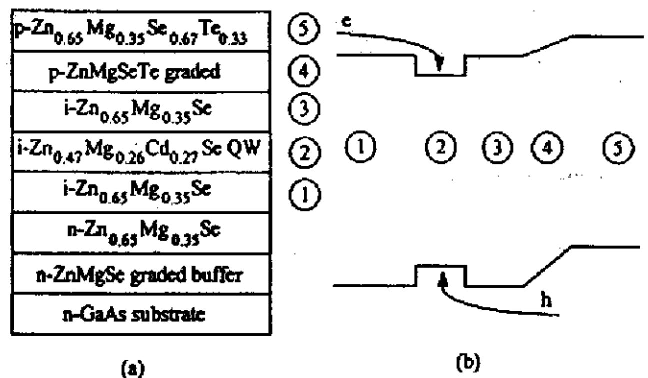

Fig.7. (a) device structure and (b) band diagram under flat band conditions for the light emitting diode containing ZnMgCdSe QW.

An intrinsic ZnMgSe spacer layer, 50Å thick, was used before and after the QW, to avoid the presence of Te, that will be used in the p-side of the diode, near the active zone. since Te is thought to form deep traps in ZnSe, which are responsible for very broad and intense PL emissions [19]. After the second spacer layer, a 100Å thick graded ZnMgSeTe superlattice (SL), where the Te content was varied linearly from zero to about 30 %, was introduced to decrease the defect density near the QW. The Zn to Mg content was exactly the same as for the n-type ZnMgSe. The p-contact layer was a ZnMgSe/ZnMgTe SL with 30 %

Te. The p-type doping, also about 10^{18} cm^{-3}, was achieved using a nitrogen DC-plasma cell [6]. The active QW region has a thickness of 200Å and a composition of $Zn_{0.47}Mg_{0.26}Cd_{0.27}Se$. The contacts used were Ga-In on the GaAs substrate and Au at the p-side.

Fig. 8 shows the electroluminescence spectra of the diode under continuos wave operation at 77 K and at room temperature. The diode emits at 2.65 eV at 77 K, corresponding to a wavelength of 468 nm, which is deep in the blue range. The oscillations observed in the low energy shoulder are caused by interference effects due to internal reflections at the GaAs/ZnSe interface and the Au contact. The FWHM is 30 meV, the same value observed previously in the photoluminescence experiments with ZnMgCdSe QWs. At room temperature, the emission peak shifts approximately 100 meV to lower energies, but remains in the blue spectral range (2.55 eV, 486 nm). At the same time the FWHM increases to about 45 meV. This value is certainly too large for laser applications, but it is, at least partially, caused by the relatively low crystalline quality of the sample.

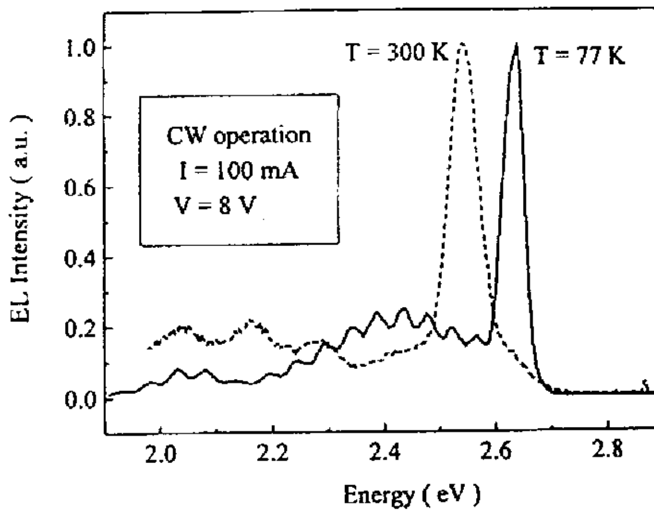

Fig.8. Elektroluminescence signal at 77K and at room temperature for the diode containing a ZnMgCdSe QW, for a CV current of 100mA.

3.3 Quantum wires and strain relaxation

The fabrication techniques for quantum wires and dots in III-V compounds are well established [20]. There has also been a lot of interest in II-VI compound quantum wires and dots, for which several etching recipes were given [21-23].

CdTe/MnTe superlattices were grown by MBE on (001) $Cd_{0.96}Zn_{0.04}Te$ substrates. The growth of the CdTe buffer layer was initiated by atomic layer epitaxy for the first 10 monolayers. This procedure ensured a perfect two dimensional growth mode, as evidenced by RHEED patterns. The superlattices with 20 periods consisted of nominally 17nm CdTe and about 2nm MnTe to achieve pseudomorphic growth. During both the CdTe and MnTe layer growth the surface was stabilized in a 2x1 reconstruction by a surplus of Te. Under these conditions the MnTe layers grow in the metastable zinkblende structure.

Periodic arrays of CdTe/MnTe multiple quantum wires were realized by holographic lithography (Ar-ion laser with a wavelength of 457.8nm) and subsequent reactive ion etching using a mixture of methane and hydrogen. The ionization of the molecules was done with a radio frequency of 13.56MHz in a plate reactor. The supplied power was 180 Watts and the acceleration voltage was 650 Volts. The etch rate of CdTe/MnTe layers was determined to be 15nm/min. Scanning electron micrographs of the etched superlattices gave quantitative information on the aspect ratio and on the steepness of the side walls, which was almost perfect.

The characterization of the etched wire structures was done by HRXD. Two dimensional maps in k-space are obtained by the independent variation of the two diffraction angels ω (between the incidence beam and the sample surface) and 2θ (between the wave vector between the incident and diffracted beams) and simultaneous recording of the diffracted x-ray intensity [24].

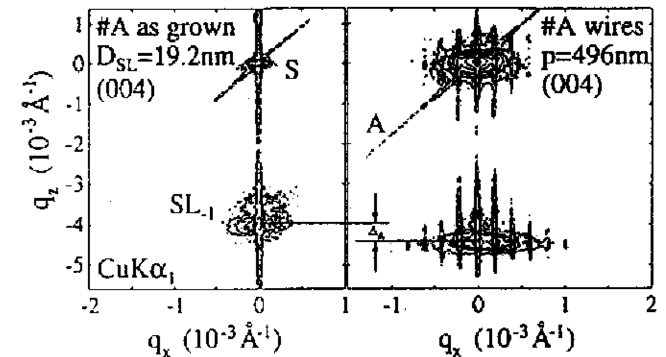

Fig. 9. Reciprocal space maps around (400) before and after the etching process of a CdTe/MnTe superlattice. The isointensity contours are plotted for 3, 6, 15, 35, 100, 500 and 1000 cps.

Double crystal ω–2θ scans of the CdTe/MnTe superlattice show peaks up to the 9th order which confirms its good crystalline quality. In Fig. 9 and 10 reciprocal space maps around the symmetric (004) and the asymmetric (115) reciprocal lattice points before and after etching are shown. "S"labels the ZnCdTe substrate peak, SL_i the superlattice peaks. W_i denotes the wire satellites of respective order and "A" is a symbol for the analyzer streak. From the spacing of the wire satellites in q_x direction, which is perpendicular both to the growth direction (q_z) and the direction of the wires (110) in real space, the wire period was determined to be 496nm.

From the reciprocal space maps we have direct evidence, that the substrate was etched, because there are wire satellites not only beside the superlattice peak SL_{-1} but also beside the substrate peak. A distinct shift of the superlattice peak in negative q_z direction is observable, which corresponds to a larger lattice constant along the growth direction in the wires with respect to the as grown superlattice. The lattice constant along the growth direction changes by 0.08% due to the patterning process. The reason for that is most probably the incorporation of hydrogen during the etching process, having in mind the rather high acceleration voltage of 650 V. This change in the lattice constant can be partly removed by annealing at a

temperature of 150°C for 15 min, which is again an indication of the hydrogen incorporation.

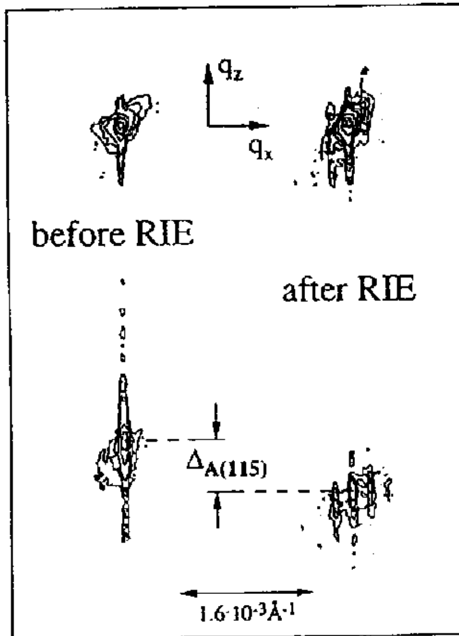

Fig. 10. Reciprocal space maps around the asymmetric (115) reflection. The scale is given by the insert arrow, which holds for both directions. The isocontours are plotted for the same intensities as in Fig.9.

From the map around the (115) reciprocal lattice point (see Fig. 10) we deduce that the in plane lattice constant of the superlattice is unchanged, since the isointensity contours of the superlattice peak with its associated wire peaks are situated exactly below the corresponding substrate peak along the (001) growth direction. These experimental findings demonstrate, that no lateral relaxation of the SL due to the wire fabrication occurs.

In the maps of the as grown samples the appearance of finite thickness fringes along the growth direction, who's spacing is indirect proportional to the total thickness of the superlattice, again demonstrate the high crystalline quality of the grown superlattices.

4. Conclusion

In conclusion, it has been shown that single layers of the quaternary system ZnMgCdSe, with controlled composition and good crystalline quality can be grown by MBE. Besides that, although an extensive study of the PL properties of ZnMgCdSe is still needed, it has been shown that very intense and relatively narrow PL emission lines can be obtained by using this quaternary system. The results of our measurements indicate that the addition of Mg to the ZnCdSe increases the band gap of the alloy, mainly due to the shift of the conduction band to higher energies, in the same way as in ZnSe. Light emitting diodes having these QWs in the active region have shown promising electrical and optical characteristics for real blue laser diodes. The device presented in this work emits at 2.55 eV at room temperature under continuos wave conditions. Reducing the Cd content in the QW to something between 10 and 20 % results in emission at energies up to 2.8 eV at room temperature.

Quantum wires were fabricated from CdTe/MnTe superlattices by reactive ion etching and analyzed by using x-rax techniques, i.e. reciprocal space mapping. This analysis yields information on the strain status of the periodic quantum wires.

Acknowledgments

The author would like to acknowledge the essential contribution of S. Ferreira, D. Stifter and M. Schmid for growing the epitaxial layers by MBE, of R. Krump for PL measurements and of H. Straub and G. Brunthaler for performing the reactive ion etching. We also want to thank O. Fuchs and E. Wirtl for technical assistance. The experimental work was supported by the "Fonds zur Förderung der wissenschaftlichen Forschung in Österreich" and by the "Jubiläumsfonds der Österreichischen Nationalbank". The basic operation of the laboratory infrastructure used was in part funded by the "Gesellschaft für Mikroelektronik".

References

[1] M.A. Haase, J. Qui, J. DePuydt, H. Cheng, Appl. Phys. Lett. **59**, 1272 (1991)
[2] J. Jeon, J. Ding, W. Patterson, A. Nurmikko, W. Xie, D. Grillo, M. Kobyashi, F.L. Gunshor, Appl. Phys. Lett. **59**, 3619 (1991)
[3] W. Faschinger, R. Krump, G. Brunthaler, S.O. Ferreira, H. Sitter, Appl. Phys. Lett. **65**, 3215 (1994)
[4] S.O. Ferreira, H.Sitter, W. Faschinger, R. Krup, G. Brunthaler, J. Crystal Growth **146**, 148 (1995)
[5] S.O. Ferreira, H. Sitter, R. Krup, W. Faschinger, Semicond. Sci. Technol. **10**, 489 (1995)
[6] W. Faschinger, S.O. Ferreira and H. Sitter, Appl. Phys. Lett. **64**, 2682 (1994)
[7] R. Krump, S.O. Ferreira, W. Faschinger, G. Brunthaler, H. Sitter, Proceedings of the European Conference on II-VI compounds (1994), World Scientific(1995)
[8] S.O. Ferreira, H. Sitter, R. Krump, W. Faschinger, G. Brunthaler, J. Crystal Growth, **159**, 640 (1996)
[9] H. Straub, G. Brunthaler, W. Faschinger, G. Bauer, Acta Physica Polonica A, **90**, 1085 (1996)
[10] A.A. Darhuber, E. Koppensteiner, H. Straub, G. Brunthaler, W. Faschinger, G. Bauer, J. Appl. Phys. **76**, 7816 (1994)
[11] E. Wirtl, H. Straub, M. Schmid, H. Sitter, P. Bauer, G. Brunthaler, J. Crystal Growth **159**, 746 (1996)
[12] E. Wirtl, H. Sitter, P. Bauer, Material Science B, Proceedings of EXMATEC, Freiburg (1995)
[13] M. A. Herman, H. Sitter, " Molecular Beam Epitaxy", 2nd revised edition, Springer Series in Material Science Vol.7 (Springer 1996)
[14] D. J. Chadi, Phys. Rev. Lett. **72**, 34 (1994)
[15] J. O. McCaldin, T.C. McGill and C.A. Mead, Phys. Rev. Lett. **36**, 56 (1976)
[16] Y. Rajakarunanayake, R. H. Miles, G.Y. Yu, T.C. McGill, Phys. Rev. **B37**, 10212 (1988)
[17] H. Okuyama, K. Nakano, T. Miyajima, K. Akimoto, Jap. J. Appl. Phys.,**30(9B)**, L1620,(1991)

[18] S.O. Ferreira, H. Sitter, W. Faschinger, Appl. Phys. Lett., **66**,1518 (1995)
[19] D. Lee, A. Mysyrowiczs, A. V. Nurmikko, B. J. Fitzpatrick, Phys. Rev. Lett., **58**, 1475 (1987)
[20] D. Heitmann, T. Demel, P. Grambow, M. Kohl, K. Ploog, in " Highlights in Condensed Matter Physics and Future Prospects", Ed. L. Esaki, Plenum Press, New York (1991)
[21] W. Walecki, W. R. Patterson, A. V. Nurmikko, H. Luo, N. Samarth, J.K. Furdyna, M. Kobayashi, S. Durbin, R. L. Gunshore, Appl. Phys. Lett. **57**, 2641 (1990)
[22] M. A. Foad, A. P. Smart, M. Watt, C. M. Sotomayor Torres, W. Kuhn, H. P. Wagner, H. Leiderer, S. Bauer, C. D. W. Wilkinson, W. Gebhardt, M. Razeghi, Surf. Sci. **267**, 223 (1992)
[23] C. Gourgon, B. Eriksson, Le Si Dang, H. Mariette, C. Vieu, J. Cryst. Growth, **138**, 590 (1994)
[24] V. Holy, L. Tapfer, E. Koppensteiner, G. Bauer, H. Lage, O. Brandt, K. Ploog, Appl. Phys. Lett., **63**, 3140, (1993)